HAL
open science

Raman satellites in optical scattering from a laser-ablated Mg plume

Alice Delserieys, F. Khattak, S. Sahoo, G. Gribakin, C. Lewis, D. Riley

To cite this version:

Alice Delserieys, F. Khattak, S. Sahoo, G. Gribakin, C. Lewis, et al.. Raman satellites in optical scattering from a laser-ablated Mg plume. Physical Review A : Atomic, molecular, and optical physics [1990-2015], 2008, 78 (5), 10.1103/PhysRevA.78.055404 . hal-01794692

HAL Id: hal-01794692

https://amu.hal.science/hal-01794692v1

Submitted on 7 Sep 2023

HAL is a multi-disciplinary open access archive for the deposit and dissemination of scientific research documents, whether they are published or not. The documents may come from teaching and research institutions in France or abroad, or from public or private research centers.

L'archive ouverte pluridisciplinaire **HAL**, est destinée au dépôt et à la diffusion de documents scientifiques de niveau recherche, publiés ou non, émanant des établissements d'enseignement et de recherche français ou étrangers, des laboratoires publics ou privés.

QUEEN'S UNIVERSITY BELFAST

Raman satellites in optical scattering from a laser-ablated Mg plume

Delserieys, A., Khattak, F. Y., Sahoo, S., Gribakin, G. F., Lewis, C. L. S., & Riley, D. (2008). Raman satellites in optical scattering from a laser-ablated Mg plume. *Physical Review A*, *78*(5), [055404]. https://doi.org/10.1103/PhysRevA.78.055404

Published in:
Physical Review A

Document Version:
Publisher's PDF, also known as Version of record

Queen's University Belfast - Research Portal:
Link to publication record in Queen's University Belfast Research Portal

Publisher rights
© 2008 The American Physical Society

General rights
Copyright for the publications made accessible via the Queen's University Belfast Research Portal is retained by the author(s) and / or other copyright owners and it is a condition of accessing these publications that users recognise and abide by the legal requirements associated with these rights.

Take down policy
The Research Portal is Queen's institutional repository that provides access to Queen's research output. Every effort has been made to ensure that content in the Research Portal does not infringe any person's rights, or applicable UK laws. If you discover content in the Research Portal that you believe breaches copyright or violates any law, please contact openaccess@qub.ac.uk.

Open Access
This research has been made openly available by Queen's academics and its Open Research team. We would love to hear how access to this research benefits you. – Share your feedback with us: http://go.qub.ac.uk/oa-feedback

Download date:07. Sep. 2023

Raman satellites in optical scattering from a laser-ablated Mg plume

A. Delserieys, F. Y. Khattak,* S. Sahoo, G. F. Gribakin, C. L. S. Lewis, and D. Riley
School of Mathematics and Physics, Queen's University Belfast, Belfast BT7 1NN, Northern Ireland, United Kingdom
(Received 13 June 2008; revised manuscript received 26 August 2008; published 26 November 2008)

Raman satellites have been observed in the scattering of a Nd:YAG laser (532 nm) from a laser-ablated Mg plasma plume. We identify them as originating from transitions between the fine-structure components of the metastable $3s3p\ ^3P_{0,1,2}$ level of Mg. We have calculated the cross sections for Raman and Rayleigh scattering from the metastable state. Comparison of the expected ratio of the satellites to the Rayleigh peak indicates the changing population fraction of the metastable states in the plume.

DOI: 10.1103/PhysRevA.78.055404 PACS number(s): 33.20.Fb, 79.20.Ds, 52.25.Os, 52.27.Gr

INTRODUCTION

In this work we have used photon scattering of the second harmonic of a Nd:YAG laser (532 nm) to probe a laser-produced Mg plasma. In addition to the Rayleigh peak, Raman transitions between the fine-structure levels of metastable Mg $3s3p\ ^3P$ have been observed. The relative intensities of the satellites are in good agreement with the theoretical predictions.

Consider the scattering of a photon by an electronic system [1], e.g., an atom or a molecule. If the state of the system remains unchanged, the photon is scattered elastically (Rayleigh scattering). This is a coherent process that accompanies the propagation of light through a medium. If the final state of the system is different from its initial state, the frequency of the scattered photon is shifted by the excitation energy of the system (inelastic, Raman scattering). Raman scattering is an important probe for studying solids and molecules in liquid and gas phases, in particular their vibrational, rotational, and other low-frequency modes.

Rayleigh and Raman scattering by atoms and ions affects the opacity and emission in stellar atmospheres [2,3]. Raman scattering by atoms is a diagnostic tool for high-pressure discharges [4], chemical lasers [5], and flames [6]. Raman scattering cross sections have been evaluated for transitions between levels with different principal quantum numbers in hydrogenic systems [7,8] and caesium [9], and fine-structure transitions in metallic atoms [4], oxygen [6], and halogens [5,10].

Raman scattering has been used to study particulates [11] in a laser ablated plume and for analysis of pulsed laser deposited films [12,13]. This paper reports observations of atomic Raman satellites in a laser ablated plume and we point out the potential of Raman scattering for diagnosing the relative populations of excited levels in a partially ionized plasma. This can be an important tool in benchmarking collisional radiative models, which are in turn essential for interpreting optical emission spectra.

THEORY

Consider an atom in the initial state i, which absorbs a photon with energy $\varepsilon=\hbar\omega$ and polarization vector $\mathbf{e}$, and emits a photon with energy $\varepsilon'=\hbar\omega'$ and polarization $\mathbf{e}'$, leaving the atom in the final state f. The amplitude of this process is

$$A_{fi}(\omega)=\sum_n\left[\frac{\langle f|\mathbf{e}'^*\cdot\mathbf{D}|n\rangle\langle n|\mathbf{e}\cdot\mathbf{D}|i\rangle}{E_i-E_n+\varepsilon+i0}+\frac{\langle f|\mathbf{e}\cdot\mathbf{D}|n\rangle\langle n|\mathbf{e}'^*\cdot\mathbf{D}|i\rangle}{E_i-E_n-\varepsilon'+i0}\right], \tag{1}$$

where the sum is over all intermediate states n, $\mathbf{D}$ is the dipole moment operator, E_i and E_n are the energies of the initial and intermediate states, and $\varepsilon'=E_i+\varepsilon-E_f$. The cross section for the final photon to be scattered into the solid-angle element $d\Omega'$ is then

$$d\sigma_{if}=\frac{\omega\omega'^3}{c^4}|A_{fi}(\omega)|^2d\Omega', \tag{2}$$

where c is the speed of light [1].

In general, atomic eigenstates are characterized by the quantum numbers of the total angular momentum and its z component, so that $|i\rangle\equiv|\gamma JM\rangle$, $|f\rangle\equiv|\gamma' J'M'\rangle$ and $|n\rangle\equiv|\gamma_n J_n M_n\rangle$, where γ, γ', and γ_n stand for all other quantum numbers of the initial, final and intermediate states, respectively. Expanding the polarization and dipole moment vectors in spherical basis components, we can use standard angular momentum algebra to sum over the angular momentum projections [14,15] in Eq. (1). For nonoriented atoms, cross section (2) should be averaged over $2J+1$ initial values of M and summed over $2J'+1$ degenerate sublevels M', yielding

$$\frac{d\sigma_{\gamma J\gamma' J'}}{d\Omega'}=\frac{\omega\omega'^3}{3c^4}\frac{1}{2J+1}\left[|A^{(0)}_{\gamma' J'\gamma J}(\omega)|^2|\mathbf{e}'^*\cdot\mathbf{e}|^2+\frac{3}{2}|A^{(1)}_{\gamma' J'\gamma J}(\omega)|^2(1-|\mathbf{e}'\cdot\mathbf{e}|^2)+\frac{3}{2}|A^{(2)}_{\gamma' J'\gamma J}(\omega)|^2\left(1+|\mathbf{e}'\cdot\mathbf{e}|^2-\frac{2}{3}|\mathbf{e}'^*\cdot\mathbf{e}|^2\right)\right], \tag{3}$$

where

*Currently at: Department of Physics, Kohat University of Science and Technology, Kohat-26000, NWFP, Pakistan.

 ©2008 The American Physical Society

$$A^{(\kappa)}_{\gamma' J' \gamma J}(\omega) = (-1)^{J+J'+\kappa} \sum_n \begin{Bmatrix} J & J' & \kappa \\ 1 & 1 & J_n \end{Bmatrix} \times \langle \gamma' J' \| D \| \gamma_n J_n \rangle \langle \gamma_n J_n \| D \| \gamma J \rangle \times \left[\frac{1}{E_{\gamma J} - E_{\gamma_n J_n} + \varepsilon + i0} + \frac{(-1)^\kappa}{E_{\gamma J} - E_{\gamma_n J_n} - \varepsilon' + i0} \right] \tag{4}$$

is the reduced matrix element of the irreducible tensor of rank $\kappa = 0,1,2$, constructed from two rank-1 dipole matrix elements [16] and $\langle \cdots \| D \| \cdots \rangle$ are the reduced dipole matrix elements [15].

The cross section (3) has the form of Eq. (60.7) of Ref. [1], the terms in square brackets corresponding to scalar ($\kappa=0$), antisymmetric ($\kappa=1$), and symmetric ($\kappa=2$) scattering. It gives the cross section of polarized ($\mathbf{e}'=\mathbf{e}$) or depolarized ($\mathbf{e}' \cdot \mathbf{e}=0$) scattering. Their sum corresponds to scattering at 90° to the incident beam direction and polarization, summed over the final photon polarizations. Equation (3) yields the total cross section integrated over the directions and summed over the polarizations of the final photon

$$\sigma_{\gamma J \gamma' J'} = \frac{8\pi\omega\omega'^3}{9c^4(2J+1)} \sum_{\kappa=0}^{2} (2\kappa+1) |A^{(\kappa)}_{\gamma' J' \gamma J}(\omega)|^2. \tag{5}$$

The eigenstates of lighter atoms and ions can be described using LS coupling, with J enumerating the components of fine-structure multiplets. In this approximation the dipole matrix elements are given by Eq. (9.63) of Ref. [15]. Neglecting the fine-structure splitting of the intermediate states, and considering nonresonant processes (i.e., nonzero energy denominators), one obtains

$$A^{(\kappa)}_{\gamma' J' \gamma J}(\omega) = (-1)^{J+S-L'} \Pi_{JJ'} \begin{Bmatrix} S & L' & J' \\ \kappa & J & L \end{Bmatrix} \times \sum_n \begin{Bmatrix} L & L' & \kappa \\ 1 & 1 & L_n \end{Bmatrix} \langle \gamma' L' \| D \| \gamma_n L_n \rangle \langle \gamma_n L_n \| D \| \gamma L \rangle \times \left[\frac{1}{E_{\gamma J} - E_{\gamma_n L_n} + \varepsilon} + \frac{(-1)^\kappa}{E_{\gamma J} - E_{\gamma_n L_n} - \varepsilon'} \right], \tag{6}$$

where $\Pi_{JJ'} = \sqrt{(2J'+1)(2J+1)}$, and the initial ($\gamma L$), final ($\gamma' L'$) and intermediate ($\gamma_n L_n$) states have the same spin S. If the fine structure of the Raman transitions is not resolved, the total photon scattering cross section between the levels γLS and $\gamma' L' S$ is given by

$$\bar{\sigma}_{\gamma L \gamma' L'} = \frac{\Sigma_{J,J'} (2J+1) \sigma_{\gamma J \gamma' J'}}{(2L+1)(2S+1)}, \tag{7}$$

where $\sigma_{\gamma J \gamma' J'}$ is obtained using Eq. (6), and similarly for the differential cross section. The relative intensities of the Raman lines between the components of the multiplet are found as $I_{JJ'} = (2J+1)\sigma_{\gamma J \gamma' J'} / \bar{\sigma}_{\gamma L \gamma' L'}$, so that $I_{JJ'} = I_{J'J}$ and $\Sigma_{J,J'} I_{JJ'} = 1$.

TABLE I. Energies and reduced dipole matrix elements of dominant low-energy transitions in Mg and Mg$^+$.

γLS	$E_{\gamma LS}$ (eV)	$\gamma_n L_n S$	$E_{\gamma_n L_n S}$ (eV)	$\langle \gamma_n L_n \| D \| \gamma L \rangle$[a] (a.u.)
Mg $3s^2\ ^1S$	0.0	$3s3p\ ^1P$	4.346	4.05
		$3s4p\ ^1P$	6.118	0.86
Mg $3s3p\ ^3P$	2.714[b]	$3s4s\ ^3S$	5.108	2.65
		$3s3d\ ^3D$	5.946	4.85
		$3s4d\ ^3D$	6.719	2.07
		$3p^2\ ^3P$	7.173	4.06
Mg$^+$ $3s\ ^2S$	0.0	$3p\ ^2P$	4.431	2.91

[a]Obtained using oscillator strengths from Refs. [17,18].
[b]This value is the average over the fine-structure multiplet at 21 850.41, 21 870.46, and 21 911.18 cm^{-1} for J=0, 1, and 2, respectively [17].

CALCULATIONS FOR Mg

To aid the analysis of the experiment, we calculate the Rayleigh and Raman cross sections for the ground ($3s^2\ ^1S_0$) and metastable ($3s3p\ ^3P_J$) states of Mg and for Mg$^+$ $3s\ ^2S_{1/2}$ for the initial photon energy ε=2.33 eV. It is known from Mg photoabsorption data that the strongest lines involve single-electron $3s \to 3p$ and $3p \to 3d$ transitions [17]. This allows us to evaluate the cross sections by using only a small number of low-lying intermediate states. Their energies are known from experiment, and the reduced dipole matrix elements are found from experimental and accurate theoretical oscillator strengths (Table I).

The differential cross sections calculated for parallel polarization and for scattering at 90°, and the total cross sections averaged over the fine-structure components are given in Table II. The cross sections for ground-state Mg are about four times greater than those of Mg$^+$. The cross sections for metastable Mg $3s3p\ ^3P$ are two orders of magnitude greater than those of Mg $3s^2$. This difference is due to the fact that for Mg $3s3p\ ^3P$, the contributions of the $3s4s\ ^3S$ intermediate state, and to a lesser degree, $3s3d\ ^3D$ state, are strongly enhanced due to small energy denominators.

Table III and Fig. 1 show the relative intensities of transitions between the fine-structure components of Mg $3s3p\ ^3P_J$. The distribution of intensities between the Rayleigh and Raman peaks depends on the cross section mea-

TABLE II. Rayleigh scattering cross sections from ground-state Mg and Mg$^+$, and multiplet-averaged Rayleigh and Raman cross sections for the metastable state Mg $3s3p\ ^3P$ for $\hbar\omega$=2.33 eV.

State	$d\sigma/d\Omega'$[a] (cm^2 sr^{-1})	$d\sigma/d\Omega'$[b] (cm^2 sr^{-1})	$\bar{\sigma}$ cm^2
Mg$^+$ $3s\ ^2S$	0.98×10^{-26}	0.98×10^{-26}	0.82×10^{-25}
Mg $3s^2\ ^1S$	4.15×10^{-26}	4.15×10^{-26}	3.48×10^{-25}
Mg $3s3p\ ^3P$	1.87×10^{-24}	3.15×10^{-24}	3.70×10^{-23}

[a]Parallel polarization.
[b]Scattering at 90°, summed over final photon polarization.

TABLE III. Relative intensities of Rayleigh and Raman transitions between the fine-structure sublevels of Mg $3s3p\ ^3P_J$ in differential and total scattering for $\hbar\omega$=2.33 eV.

$J-J'$	0-0	0-1	0-2	1-1	1-2	2-2
$e'=e$[a]	0.056	0.000	0.056	0.208	0.125	0.375
90°, sum[b]	0.033	0.020	0.058	0.158	0.155	0.342
Total[c]	0.024	0.029	0.059	0.136	0.168	0.329

[a]Parallel polarization.
[b]Scattering at 90°, summed over final photon polarization.
[c]Total scattering summed over final photon polarization.

sured. In particular, in polarized scattering the intensity of the 0-1 transition is exactly zero. Indeed, for $J=0$ and $J'=1$, the $6j$ symbol in Eq. (4) is nonzero only for $\kappa=1$, but the contribution of asymmetric scattering for $\mathbf{e}'=\mathbf{e}$ vanishes. The ratios between the two strongest Raman satellites (1-2 and 0-2) in polarized 90°, and total cross sections are 2.23, 2.67, and 2.85, respectively.

EXPERIMENT

Our experimental setup has been described in an earlier paper [19]. In summary, a plasma plume is created with a KrF laser (Lambda Physik LPX 210i) of 20 ns full width half maximum duration at 248 nm. Random phase plates [20] are used with a pair of cylindrical lenses to create a 1 mm^2 spot resulting in ~9 J cm^{-2} onto a rotating Mg block. A frequency doubled Nd:YAG pulsed laser (9 ns, 400 mJ at 532 nm) is used to probe a slice of the plume at a predetermined distance from the target surface at controlled delays ranging from 100 ns to 1 μs.

The probe is slightly focused (f/200) to ~0.5 mm FWHM. The scattered radiation at 90° is focused into the slit of a double grating spectrometer (SPEX 750 spectrometer, focal length 0.75 m, 1200 lines/mm gratings) with a dispersion of 5.7 Å/mm. The spectrometer is fitted with an Andor Instaspec V ICCD camera (1024×256 pixels of 26 μm square coupled to an MCP [21]) with a 10 ns gate, synchronised to collect the scatter signal and allowing a great reduction in detected plasma self emission. The chamber was

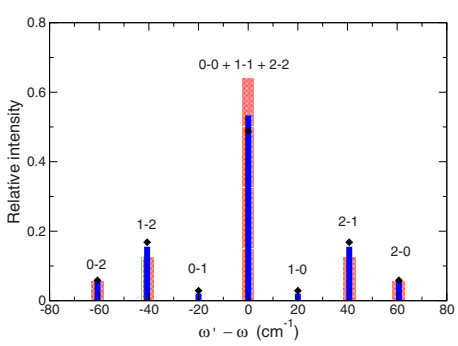

FIG. 1. (Color online) Intensities of transitions between the fine-structure sublevels of Mg $3s3p\ ^3P_J$ for $\hbar\omega$=2.33 eV. Wide bars, polarized scattering; narrow bars, scattering at 90°, summed over final photon polarization; diamonds, total scattering.

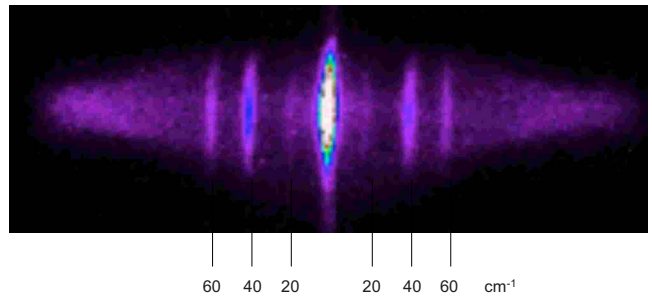

FIG. 2. (Color online) Top: raw image with 500 shots accumulated, plasma probed at 2 mm from target surface, 200 ns delay. The satellites are indicated by the shift markers.

equipped with opaque materials and apparatus to reduce the stray light. The scattering signal, such as that shown in Fig. 2, was averaged over ~500 shots with the lasers running at 10 Hz. The Raman satellites are clearly visible at 20, 40, and 60 cm^{-1} on either side of the central Rayleigh peak. Underlying the satellites, is the free electron Thomson scatter data which has been analyzed and presented separately [19]. In this case, the fit to the Thomson scatter data indicates an electron density ~9.5×10^{16} cm^{-3} and electron temperature of 1.7 eV. For plasma at this density and temperature, we expect populations to be close to local thermodynamic equilibrium (LTE) [22], with average ionization ~0.4 and the population of the metastable level about 1.8 times the ground state population.

In Fig. 3(a) we show the experimental signals of the Rayleigh peak and 2-1, 1-2, 2-0, and 0-2 satellites as a function of time at 2 mm from the target surface. Figure 3(b) shows the ratio of the strongest Raman satellite at $\omega'-\omega=\pm40$ cm^{-1} to the Rayleigh peak at 2 mm from the target. When the spectrometer response with polarization is ac-

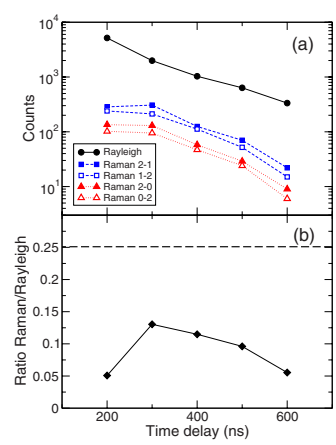

FIG. 3. (Color online) (a) Experimental signal in the Rayleigh peak (circles) and Raman Stokes, 2-1 (solid squares), 2-0 (solid triangles), and anti-Stokes satellites, 1-2 (open squares), 0-2 (open triangles), as a function of the time delay between the KrF and Nd:YAG laser pulses. (b) Ratio of the average of Stokes and anti-Stokes satellites at 40 cm^{-1} from the central wave number to the Rayleigh peak (diamonds). The dashed line shows the expected ratio for scattering from the metastable atoms, taking into account the spectrometer polarization efficiency.

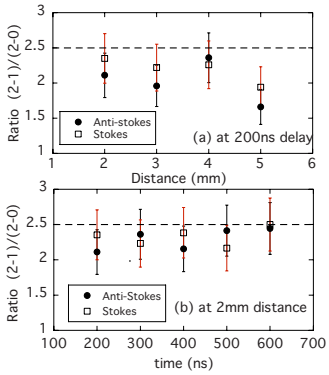

FIG. 4. (Color online) (a) Ratio of 2-1 to 2-0 satellites as a function of delay at 2 mm from the target surface. (b) Same as (a) but as a function of distance from target at delay 200 ns. The dotted lines show the expected ratio.

counted for, we expect the Rayleigh peak for the Mg ground state to be about 60 times smaller than for the metastable state, and we expect the ratio of Raman to Rayleigh peaks to be dominated by the ratio expected for the metastable state, which for the ± 40 cm^{-1} case is approximately 0.25. As we can see, the ratio starts off lower and grows to about 50% of this value and then drops again.

We can interpret this result as meaning that at early time, the plume is more highly ionized and the Rayleigh signal has a significant contribution from Mg II ions. As recombination leads to a higher metastable Mg I population, the ratio of Raman to Rayleigh increases. At later times, with lower density, the metastables may be depopulated by excitation to higher states such as the $3s4p\ ^1P$, which then has a fast radiative decay to the ground state. However, the ratios indicate that the metastable has a lower population than would be suggested by LTE. If we assume that, at late time, the plume is mostly neutral, we can use the calculated Rayleigh cross sections to estimate that the metastable population is only $\sim 2\%$ of the ground-state population. Expansion of the plume to lower density means that we are further from LTE. However, the metastable state has a 3.9 ms radiative decay lifetime and it is clear that we need some more sophisticated time dependent collisional-radiative modeling with all processes, including dielectronic recombination accounted for.

The experimental ratio of the strongest satellite (2-1, 1-2) at ± 40 cm^{-1} of the central line to the second strongest satellite (2-0, 0-2) at ± 60 cm^{-1} was measured at several delays and distances from the target surface. This can be seen in Fig. 4 and was quite consistent, with values close to the ratio 2.50 expected. The 0-1 and 1-0 satellites at ± 20 cm^{-1} of the Rayleigh peak are weak but clearly visible. Their ratio to the 0-2 and 2-0 satellites in Fig. 2 is $\sim 0.36 \pm 0.03$, whereas the expected ratio is 0.22. The data, however, are much noisier for these satellites as they are close to the strong Rayleigh peak.

SUMMARY

We have reported the observation of atomic Raman satellites in a laser produced Mg plume. Investigation of the ratio of the satellites to the Rayleigh peak indicates the changing population fraction of the metastable magnesium atoms in the plume.

ACKNOWLEDGMENTS

We thank Dr T. Field and Professor W. G. Graham for useful discussions. A.D. was supported by the European Social Fund.

[1] V. B. Berestetskii, E. M. Lifshitz, and L. P. Pitaevskii, *Quantum Electrodynamics* (Pergamon, Oxford, 1982), Chap. IV.
[2] H. Isliker, H. Nussbaumer, and M. Vogel, Astron. Astrophys. **219**, 271 (1989).
[3] H. M. Schmid, Mon. Not. R. Astron. Soc. **282**, 511 (1996).
[4] L. Vriens and M. Adriaansz, J. Appl. Phys. **46**, 3146 (1975).
[5] H. Schlossberg, J. Appl. Phys. **47**, 2044 (1976).
[6] C. J. Dasch and J. H. Bechtel, Opt. Lett. **6**, 36 (1981).
[7] L. P. Rapoport and B. A. Zon, Phys. Lett. **26**, 564 (1968).
[8] W. M. Saslow and D. L. Mills, Phys. Rev. **187**, 1025 (1969).
[9] H. R. Sadeghpour and A. Dalgarno, J. Phys. B **25**, 4801 (1992).
[10] K. Drühl, Phys. Rev. A **26**, 863 (1982).
[11] D. W. Hahn, M. N. Ediger, and G. H. Pettit, J. Appl. Phys. **77**, 2759 (1995).
[12] B. R. Mehta and E. A. Ogryzlo, Surf. Coat. Technol. **43-44**, 80 (1990).
[13] J. D. Busbee, B. Igelnik, D. Liptak, R. R. Biggers, and I. Maartense, Eng. Applic. Artif. Intell. **11**, 637 (1998).
[14] D. A. Varshalovich, A. N. Moskalev, and V. K. Khersonskii, *Quantum Theory of Angular Momentum* (World Scientific, Singapore, 1988).
[15] I. I. Sobelman, *Atomic Spectra and Radiative Transitions*, 2nd ed. (Springer, Berlin, 1992).
[16] Equation (4) is equivalent to Eq. (1.7) of Ref. [10]. The phase factor $(-1)^{J+J'+\kappa}$ ensures that for a diagonal transition, $A^{(0)}_{\gamma J \gamma J}(\omega) = \sqrt{3(2J+1)}\alpha(\omega)$, where $\alpha(\omega)$ is the dipole polarizability of state γJ, Eq. (9.49) of Ref. [15]. Note also that $\langle \gamma J \| D \| \gamma_n J_n \rangle = (-1)^{J_n - J} \langle \gamma_n J_n \| D \| \gamma J \rangle^*$.
[17] A. A. Radtsig and B. M. Smirnov, *Parameters of Atoms and Atomic Ions: Handbook* (Energoatomizdat, Moscow, 1986); Yu. Ralchenko, A. E. Kramida, J. Reader, and NIST ASD Team, NIST Atomic Spectra Database, National Institute of Standards and Technology, Gaithersburg, MD, see http://physics.nist.gov/PhysRefData/
[18] J. Mitroy and J.-Y. Zhang, Phys. Rev. A **76**, 062703 (2007), see Table VI and references therein.
[19] A. Delserieys *et al.*, Appl. Phys. Lett. **92**, 011502 (2008).
[20] C. L. S. Lewis *et al.*, Rev. Sci. Instrum. **70**, 2116 (1999).
[21] see www.andor-tech.com for manufacturer details
[22] H. R. Griem, *Principles of Plasma Spectroscopy* (Cambridge University Press, Cambridge, 1997).